PII: S0032-3861(97)00006-2

Polymer Vol. 38 No. 19, pp. 4855–4862, 1997

0032-3861/97/$17.00+0.00

Phase diagram prediction for thermoset/thermoplastic polymer blends

Stavros Elliniadis and Julia S. Higgins*
Department of Chemical Engineering, Imperial College, London SW7 2BY, UK

and Nigel Clarke and Thomas C. B. McLeish
Department of Physics and Polymer IRC, University of Leeds LS2 9JT, UK

and Riaz A. Choudhery
ICI Paints, Wexham Road, Slough, Berkshire SL2 5DS, UK

and Stephen D. Jenkins
ICI Wilton Research Centre, PO Box 90, Wilton, Middlesbrough, Cleveland TS6 8JE, UK
(Received 10 December 1996)

By performing a series of experiments on a thermoset/thermoplastic blend of epoxy/polyarylsulfone thermoplastic we are able to characterize many important parameters of the components and their interactions. We pay particular attention to the competition between phase separation and cross-linking of the epoxy, which makes these systems technologically important but complex. Using small-angle neutron scattering we determine an effective Flory–Huggins interaction parameter as a function of the temperature and the molecular weight distribution of each component, which is determined by gel permeation chromatography. These results are then incorporated into a recent model for linear/branched polymer blends to predict the evolution of phase diagrams under isothermal cure. Small-angle light scattering and scanning electron microscopy show morphologies in close agreement with the model. © 1997 Elsevier Science Ltd.

(Keywords: epoxy; polyarylsulfone; phase separation)

INTRODUCTION

Polymer blends containing a thermoset component tend to be multiphase systems with morphology controlling their performance, especially in terms of mechanical properties[1–3]. Understanding and controlling the phase separation process in such systems is, therefore, very important, particularly in the case of critical fibre–composite applications. In blends of thermoplastics, phase separation is usually induced by a temperature jump into an immiscible region. Here, however, phase separation is effectively induced by a 'chemical jump' as the molecular weight of the thermoset (i.e. epoxy) increases during isothermal cure. Depending on whether the blend is in the metastable or the unstable part of the immiscible region, phase separation will proceed via nucleation and growth or spinodal decomposition. In the first case, small concentration fluctuations will not cause the system to phase separate, as a thermodynamic barrier to phase growth needs to be overcome with a large concentration fluctuation. This fluctuation is called a nucleus: once a nucleus is formed it grows by a normal diffusion process[4]. In the second case the system is unstable to infinitesimal composition fluctuations, as there is no barrier to phase growth: thus the system separates via a spontaneous process that involves a diffusional flux against the concentration gradient[5,6]. When the phase separation mechanism is spinodal decomposition, a highly interconnected two-phase morphology with uniform domain size ('modulated structure') develops[7]. In the early stages of this process the wavelength (domain size) remains constant while the amplitude (concentration difference) of the composition fluctuation increases. In the intermediate stage both the wavelength and the amplitude increase with time. In the final stages the concentration difference between the two phases reaches its final value while the domains continue to coarsen[8]. The final morphology in thermoset/thermoplastic blends is, in fact, a result of the competition between phase separation and the accompanying chemical cross-linking, which ultimately 'locks' the structure of the blend. The complexity of this phase separation behaviour has led to a limited number of theoretical attempts to predict the evolution of the phase diagram during cure. Among others, Binder[9] and Williams[10] have modelled a thermoplastic in a weakly cross-linked network and a linear/branched blend, respectively. Clarke *et al.*[11] have utilized the Flory–Huggins theory, which was modified to account for polydispersity by Konigsveld[12] and Solc[13,14], to calculate the phase diagram of a thermoset/thermoplastic blend prior to the gel point. One of the main advantages of this

* To whom correspondence should be addressed

particular model is that it permits calculation of the coexisting phase compositions. In such an approach the complex ternary mixture of thermoplastic, epoxy and curing agent is treated as a binary blend, consisting of a monodisperse thermoplastic component, and a polydisperse epoxy and curing agent 'pseudocomponent' (so called because we describe the interaction of this copolymer with the thermoplastic by a single parameter). Although the model does not explicitly predict the evolution of the phase diagram as curing progresses, this can be effectively incorporated by allowing for different molecular weight distributions of the pseudocomponent at different times. Thus it is possible to obtain a series of 'snapshots' of the phase diagram during curing. Using the interaction parameter measured from small-angle neutron-scattering (SANS) experiments, and the molecular weight distribution of the epoxy obtained through gel permeation chromatography (g.p.c.) it was possible to use this model to predict the phase diagram for the thermoset/thermoplastic blend used here. The accuracy of these predictions was investigated through a series of small-angle light-scattering (SALS) and scanning electron microscope (SEM) experiments.

MODEL FOR PHASE SEPARATION

The major assumptions of Clarke's model are[11]:

(1) The cross-linking pseudocomponent is a polydisperse branched polymer following power law statistics, with lower and upper cut-offs N_1 and N_2, respectively,

$$\phi(N) = kN^{-(\tau-1)} \qquad N_1 < N < N_2 \tag{1}$$

where $\phi(N)$ is the volume fraction of a molecular species of the pseudocomponent with a degree of polymerization N, k is a normalization constant and τ is the critical exponent[15]. Thus $\tau = 2.5$ for classical theory[16], and $\tau = 2.2$ for percolation theory[17]. In this work we assume classical statistics.

(2) The thermoplastic component consists of monodisperse linear polymers.

(3) For each calculation of the phase diagram the mixture is assumed to be chemically stable.

(4) Interactions between components remain the same throughout the cross-linking process, i.e. they are independent of branched polymer composition.

The Flory–Huggins free energy of mixing of a linear/branched polymer may be written as[11,18]

$$\frac{F_{mix}}{k_B T} = \frac{\phi_{lin}}{N_{lin}} \ln \phi_{lin} + \sum_i \left(\frac{\phi_i}{N_i} \ln \phi_i \right) + \chi \phi_{lin}(1 - \phi_{lin}) \tag{2}$$

where the ith component of the branched polymer has volume fraction ϕ_i and a degree of polymerization N_i, ϕ_{lin} is the volume fraction of the thermoplastic (linear) component, F_{mix} is the Helmholtz free energy of mixing per lattice site, χ is the interaction parameter between the thermoplastic component and the epoxy–amine (branched) pseudocomponent. We define

$$n_i = \frac{N_i}{N_{lin}} \qquad i = 1, 2 \tag{3}$$

It is possible to derive simple expressions for the reduced n, w and z polydispersity averages ($\overline{n_n}$, $\overline{n_w}$, $\overline{n_z}$) of the branched (epoxy–amine) component[11].

The model[19] may then be solved for the spinodal curve and critical point in terms of the above molecular weight averages, which in turn depend on the degree of cross-linking (up to the gel point). The spinodal curve is given by

$$N_{lin}\chi_s = \frac{1}{2}\left(\frac{1}{\phi_{lin}} + \frac{1}{(1 - \phi_{lin})\overline{n_w}} \right) \tag{4}$$

and the critical point by

$$\phi_{lin}^{crit} = \left(1 + \frac{\overline{n_z}^{1/2}}{\overline{n_w}} \right)^{-1} \qquad N_{lin}\chi_s^{crit} = \frac{1}{2}\left(\frac{1}{\phi_{lin}^{crit}} + \frac{1}{(1 - \phi_{lin}^{crit})\overline{n_w}} \right) \tag{5}$$

Due to the polydispersity of the pseudocomponent for each blend composition there is a unique set of coexistence curves for the emerging phases, which do not coincide with the cloud point curve (which delineates the limit of stability of the one phase region). These are calculated by simultaneously solving the following equations, which can be derived from the condition that the chemical potential of each component in each phase is equal:

$$\ln \phi'_{lin} + (1 - \phi'_{lin})\left(1 - \frac{1}{\overline{n_n}'}\right) + N_{lin}\chi(1 - \phi'_{lin})^2 = \ln \phi''_{lin} + (1 - \phi''_{lin})\left(1 - \frac{1}{\overline{n_n}''}\right) + N_{lin}\chi(1 - \phi''_{lin})^2 \tag{6}$$

and

$$\frac{V''}{V}(1 - \phi''_{lin}) = \frac{(\tau - 2)(1 - \phi''_{lin})}{n_1^{-(\tau-2)} - n_2^{-(\tau-2)}} \int_{n_1}^{n_2} \frac{n^{-(\tau-1)}}{1 + re^{\sigma n}} dn$$

at various $N_{lin}\chi$ for fixed ϕ_{lin}, n_1 and n_2. In equations (6) the following parameters have been defined:

$$\sigma = 2N_{lin}\chi(\phi''_{lin} - \phi'_{lin}) + \ln\left(\frac{\phi'_{lin}}{\phi''_{lin}} \right)$$

and

$$r = \frac{V'}{V''}$$

Single and double primes denote the branch-rich and linear-rich phases, respectively, while V is the total volume.

The cloud point curve, for which the principal phase has the same characteristics as the bulk, is calculated by

$$\frac{\sigma}{2}(1 + \nu_0) + \left(1 - \frac{1}{\overline{n_n}}\right) - \nu_0\left(1 - \frac{1}{\overline{n_n}'''}\right) + \left(\frac{1}{1 - \phi_{lin}} - \frac{1 - \nu_0}{2} \right) \ln\left(\frac{\phi_{lin}}{\phi'''_{lin}} \right) = 0$$

$$\nu_0 = \frac{(1 - \phi'''_{lin})}{(1 - \phi_{lin})} N_{lin}\chi = \frac{\sigma - \ln(\phi_{lin}/\phi'''_{lin})}{2(\phi'''_{lin} - \phi_{lin})} \tag{7}$$

The parameters of the incipient phase are denoted by triple primes, while those of the principal phase are without primes.

The spinodal curve and critical point are calculated analytically from equations (4) and (5), while the coexistence conditions and cloud point curves are obtained numerically from equations (6) and (7), respectively.

It is evident from the above that in order to be able to predict the familiar temperature–composition phase diagram one needs the molecular weight of the linear component, the molecular weight distribution (MWD) of the pseudocomponent, and the temperature dependence of the χ parameter for the system. Furthermore, to predict the evolution of the phase diagram under cure, the MWD for the pseudocomponent at different times during the curing process must be known. In particular, we need some estimation of the upper and lower cut-offs for the branched polymer. A similar model has recently been used by Riccardi *et al.*[20] to study the phase behaviour of linear/branched blends. They adopted Flory–Stockmayer statistics for the distribution function of the branched polymer[21,22]. The expression that we have adopted, equation (1), is an approximation of the above statistics, which has been shown to be a good representation[23], particularly for $n_2/n_1 \gg 1$. The most drastic approximation inherent in equation (1) is the lower cut-off; however, we do not believe this significantly affects the theoretical predictions, as the most interesting phenomena associated with these blends occur due to the variation of n_2[11]. Also, equation (1) enables us to write explicit and simple expressions for the spinodal, critical point and polydispersity averages, as well as being a good approximation to Flory–Stockmayers statistics.

NEUTRON SCATTERING

The SANS method[24,25] has been successfully used to measure the interaction parameter, in the one-phase region, of blends containing one deuterated component[26–31]. The magnitude of the scattering vector $\boldsymbol{q}$ is

$$q = \frac{2\pi}{\lambda}\sin\frac{\theta}{2} \tag{8}$$

where θ is the scattering angle and λ is the wavelength of the scattered beam*. According to Higgins *et al.*[32] the absolute coherent elastic scattering cross-section, $d\sigma(q)/d\Omega$, for a one-phase mixture of two components is

$$\frac{d\sigma(q)}{d\Omega} = \frac{(b_1 - \beta b_2)^2 S(q)}{V_1} \tag{9}$$

where V_i is the volume of the repeat unit of component i, b_i is the coherent scattering length of a repeat unit of component i, β is the ratio V_1/V_2, q is the magnitude of the scattering vector and $S(q)$ is the structure factor.

By applying the random phase approximation (RPA), which for an interacting system yields[33,34]

$$\frac{1}{S(q)} = \frac{1}{\phi_1 S_1(q)} + \frac{1}{\phi_2 S_2(q)} - 2\chi_{\text{eff}} \tag{10}$$

where ϕ_i, $S_i(q)$, are the volume fraction and structure factor, respectively, of each component, $S(q)$ is the total structure factor and χ_{eff} is an effective interaction parameter per segment mole of polymer 1, Higgins and co-workers showed[35–38] that the SANS of a homogeneous one-phase polymer blend of two components, in which one of them is deuterium labelled, is given by the equation

$$\frac{d\sigma(q)}{d\Omega} = \frac{(d - \beta b)^2}{V_1\left[\dfrac{1}{(N_1\phi_1 P_1(q)} + \dfrac{\beta}{(N_2\phi_2 P_2(q))} - 2\chi_{\text{eff}}\right]} \tag{11}$$

where $d\sigma(q)/d\Omega$ is the normalized coherent scattering as a function of q, d is the coherent scattering length of a repeat unit of the deuterated polymer, N_i is the degree of polymerization of species i and P_i is the Debye scattering function where

$$P_i(q) = \frac{2}{(u+1)v^2}\left((1+uv)^{-1/u} - 1 + v\right) \tag{12}$$

$$u = \frac{M_{w_i}}{M_{n_i}} - 1 \qquad v = \frac{R_{g_i}^2 q^2}{2u+1} \tag{13}$$

M_w, M_n are the weight average and number average molecular weights and R_g is the z average radius of gyration. In the Zimm range[39], $qR_g < 1$, the functions

$$P_i(q) \rightarrow 1 - \frac{R_{g_i}^2 q^2}{3} \tag{14}$$

Consequently, in this range the intensity should vary linearly with q^2.

Furthermore, $\lim_{q\rightarrow 0}[P(q)] = 1$, and the scattering intensity is inversely proportional to the second derivative of the Gibbs free energy of mixing per lattice site divided by $k_B T$, G''[38]:

$$\left.\frac{d\sigma(q)}{d\Omega}\right|_{q\rightarrow 0} = \frac{(d - \beta b)^2}{V_1 G''} \tag{15}$$

where

$$G'' = \frac{\partial^2(\Delta G_m/k_B T)}{\partial\phi^2} = \frac{1}{N_1\phi_1} + \frac{\beta}{N_2\phi_2} - 2\chi_{\text{eff}} \tag{16}$$

Due to equation (14) a plot of $(d\sigma(q)/d\Omega)^{-1}$ *versus* q^2 should yield a straight line, with the intercept at $q = 0$ giving the value of G'' and therefore χ_{eff}. In this approach only the degrees of polymerization and the volume fractions of the blend components need to be known.

EXPERIMENTAL

SANS measurements were made on the time-of-flight diffractometer LOQ at the ISIS pulsed neutron source at the Rutherford Appleton Laboratory in Oxfordshire, UK. Data from neutron wavelengths of 2.0–9.8 Å were combined to give a simultaneous q range of 0.006–0.22 $Å^{-1}$, at a sample detector distance of 4.4 m[40,41]. To ensure the necessary contrast for the experiment, in the polymer mixture under study, the thermoplastic, a polyarylsulfone (PAS), was replaced with a deuterium-labelled version (d-PAS) with a 64% deuteration level.

Samples were prepared as follows: the mixture of the thermoplastic (d-PAS), epoxy, Ciba Geigy MYO510 (a trifunctional epoxy based on aminophenyl and curing agent), 4,4′-diaminodiphenylsulfone (4,4′-DDS) (30/45.4/24.6 wt%) was dissolved in methylene chloride/methanol (95/5%). Drying was then carried out in the aluminium SANS cells for 30 min at 145°C under vacuum (at a pressure of 10 mbar). After drying, the samples were sealed in the SANS cells and partly cured for 17 and 30 min at 145°C, to ensure two different levels of reaction. Following part-curing, the samples were

* In SANS the wavelength of the incident beam (λ_{inc}) does not change during scattering, in SALS $\lambda = \lambda_{inc}/\mu$ where μ is the refractive index of the blend

Table 1 Annealing of blend samples containing d-PAS

Annealing temperature (°C)	Annealing time (h)
25	8
45	4
65	2
85	1
105	0.5
125	0.25

Table 2 Molecular weight of the deuterated and hydrogenous blends

	Deuterated blend		Hydrogenous blend			
				Pseudocomponent after[b]		
	d-PAS	Pseudocomponent at 145°C after 17 min	PAS	28 min	35 min	52 min
$\overline{M_w}$	5400	1880	27350	732	832	1253
M_w^{Min}	–[a]	250	–	250	250	250
M_w^{Max}	–	16000	–	5000	10000	50000

[a] The MWD of the thermoplastic was not calculated as only the average M_w is required for Clarke's model
[b] Cured as follows: placed on hot-plate at 145°C, heated at 2°C min^{-1} to 180°C and held at constant temperature for 2 h

rapidly quenched below 20°C. These quenched samples were then annealed to various temperatures for the times presented in *Table 1* in an attempt to reach equilibrium at those temperatures. After annealing, the samples were quenched again to 10°C and stored at 6°C before being irradiated with neutrons.

D.s.c. scans on the samples showed that their glass transition temperatures (T_g) were 28°C for the samples cured for 17 min, and 43°C for those cured for 30 min. To confirm that the deuterated samples were still in the one-phase region, samples of identical composition were prepared on microscope cover-slips and cured at 145°C for 2 h under light-scattering observation. The results indicated that there was no increase in the scattered intensity, which would denote phase separation, for at least 1 h, hence our samples, cured for 17 or 30 min, would not have phase separated.

In order to be able to use the theory outlined above, the molecular weight of the epoxy–amine pseudocomponent for the two series of SANS samples and its MWD with time during cure need to be known. Various studies have shown that epoxy cure kinetics is affected by the presence of polyarylsulfone thermoplastics[42–44] and the solvent preparation route that was followed[45]. Consequently, the molecular weight of the epoxy could not be accurately deduced from previous work[46]. Thus the required molecular weights were established by g.p.c.* as follows. After establishing the MWD of the deuterated thermoplastic, it was possible† to extract the MWD of the pseudocomponent from the g.p.c. graph of the deuterated blend. This exhibited a shoulder due to overlapping of the epoxy and thermoplastic g.p.c. peaks. For the pseudocomponent MWD with time, in a blend containing hydrogenous thermoplastic, a series of experiments were performed whereby samples of the cross-linking blend were taken at various times for g.p.c. analysis. By subtracting† the hydrogenous thermoplastic MWD, the pseudocomponent MWD at specific times during cure was obtained. G.p.c. curves for the various blends are presented in *Figure 1*.

Table 2 summarizes the information that was obtained through the g.p.c. experiments. Note that the values for the average molecular weight, $\overline{M}_w$, were obtained from the peak positions in the g.p.c. graphs and these values were used for the calculation of χ_{eff}[47]. Unfortunately it was not possible to analyse the deuterated samples cured for 30 min at 145°C as they were only partially soluble, due to the extent of crosslinking, hence no values of χ_{eff} could be obtained using equation (16). From the above it can be concluded that the epoxy cures faster when mixed with the low molecular weight deuterated PAS than in a blend with the higher molecular weight hydrogenous PAS, even though in the latter the curing reaction takes place at much higher temperatures.

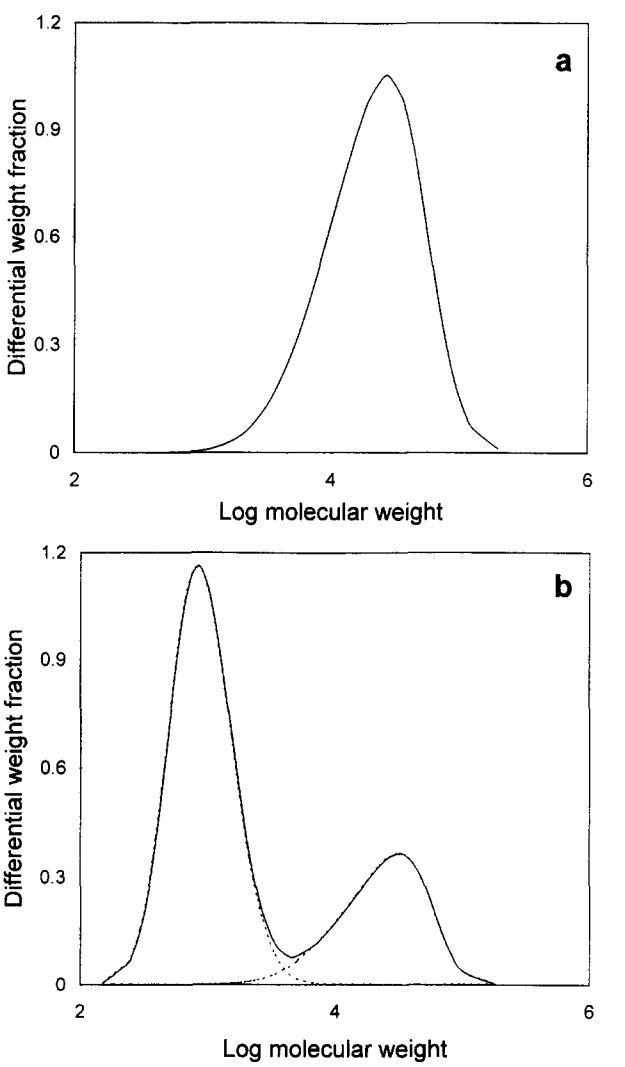

Figure 1 G.p.c. curves for (a) hydrogenous thermoplastic and (b) hydrogenous blends after 35 min

* All g.p.c. results were derived using polystyrene for calibration
† Using commercial software, PEAKFIT™ by Jandel Scientific

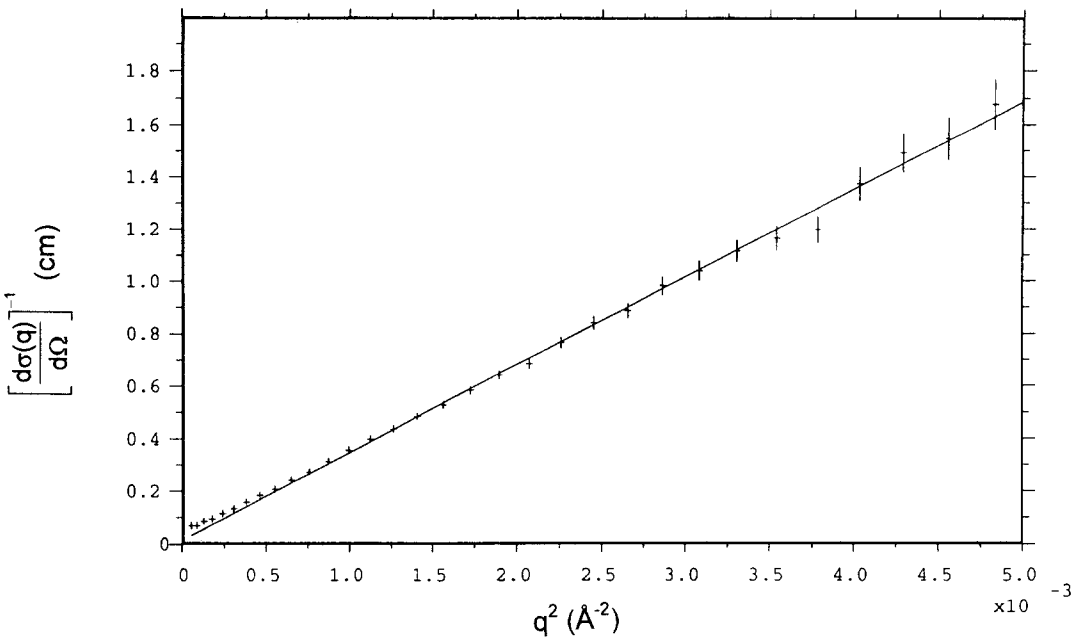

Figure 2 Inverse cross section *versus* q^2 for a deuterated blend

Table 3 Element scattering lengths

Element[atomic number]	Bound coherent scattering length (fm)[a]
H^1	−3.739
H^2	6.671
C^{12}	6.646
N^7	9.360
O^8	5.803
S^{16}	2.847

[a] 1 fm = 10^{-13} cm

The results of the neutron-scattering experiments[48] after correction for background scattering, transmission and reduction were in the form cross-section $(d\sigma(q)/d\Omega)$ (cm^{-1}) *versus* wavelength (q) $(Å^{-1})$. In all cases the parasitic scattering from the sample holder was subtracted from the sample scattering, and the incoherent scattering background was estimated from the scattering of the hydrogenous component of the blend (pseudo-component). The absolute transmission values were estimated using a mixture of hydrogenous and deuterated polystyrenes* as the standard. Using data analysis programs the data can be plotted in the form $(d\sigma(q)/d\Omega)^{-1}$ *versus* q^2. The y axis intersect of a straight line fitted to the data in *Figure 2* yielded the value of $d\sigma(q)/d\Omega|_{q\to 0}$ and therefore χ_{eff}.

In the estimation of χ_{eff} the following values were used for the density of the materials: d-PAS, 1.49 g mol^{-1}; MYO510, 1.22 g mol^{-1}; 4,4′-DDS, 1.27 g mol^{-1}. For the estimation of the scattering lengths the values in *Table 3* were used[50].

Using the above density values, $\beta = V_{thermoplastic}/V_{pseudocomponent} = 1.215$. However, in the Clarke model, the monomeric persistence lengths of the linear and branched polymers are equal[19]. So to use the model, the volume of the repeat unit of the deuterated polymer should be adjusted so that $\beta = 1$. Consequently the molecular weight of the thermoplastic repeat unit and its scattering length need to be adjusted

* Sample name GDW20, M_n = 77 400, thickness = 1.27 mm[49]

Table 4 χ temperature dependence

Annealing temperature (°C)	χ_{eff}
45	0.152
65	0.126
85	0.138
105	0.154
125	0.156

according to

$$\frac{1}{\beta} = \frac{V_1^a}{V_1} = \frac{\overline{M}_1^a}{\overline{M}_1} = \frac{d^a}{d_1} \tag{17}$$

where V_1^a, $\overline{M}_1^a$ d_1^a are, respectively, the adjusted volume, molecular weight and scattering length of the repeat unit of the thermoplastic.

Employing equations (19) and (20), the values of the interaction parameter per segment mole (χ_{eff}) in *Table 4* were obtained.

The high value of χ_{eff} for 45°C may be attributed to the sample not reaching equilibrium at that temperature in the annealing time of 4 h, thus reflecting the value of χ_{eff} of a higher temperature.

Since χ_{eff} represents unit segment interactions of polymers in a blend it is, in theory, molecular weight independent. This has been established for mixtures of high molecular weight polymers[51]. However, χ_{eff} is strongly dependent on temperature and blend composition. Assuming its temperature dependence given by equation (18), where a is the entropic term and b is the enthalpic term[11], the results of fitting this equation to the data of *Table 3* (excluding the value for 45°C) are presented in *Figure 3*:

$$\chi = a + \frac{b}{T} \tag{18}$$

CALCULATING THE PHASE DIAGRAM

By using the Clarke model, the phase diagram for the partially cured deuterated blend can be predicted as a function of χ for the determined molecular weight values. The degrees of polymerization were estimated using the

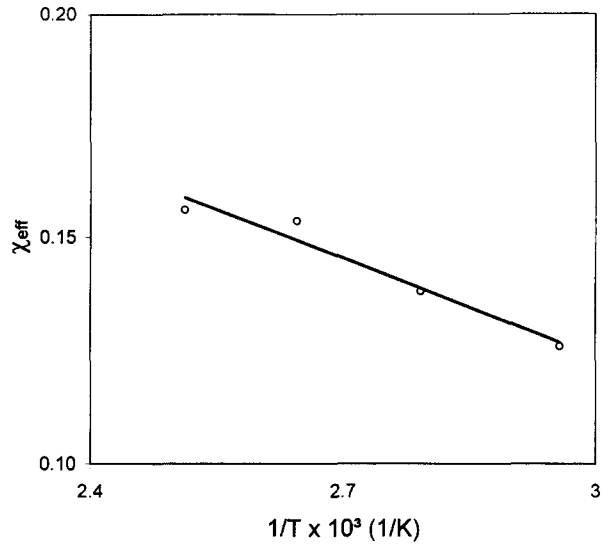

Figure 3 Temperature dependence of χ_{eff} for the deuterated blend

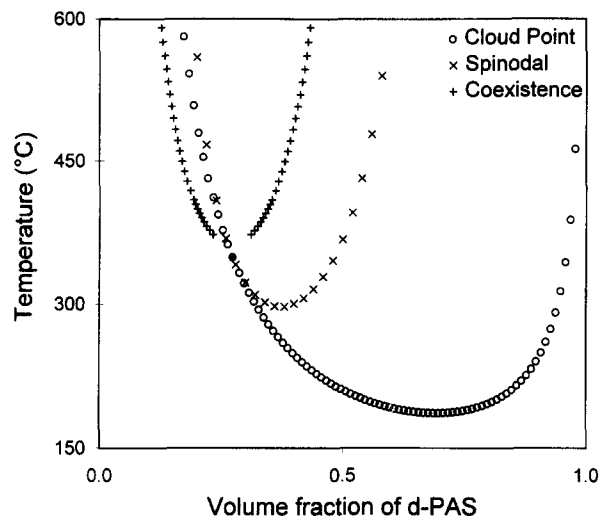

Figure 4 Estimated phase diagram for the deuterated blend. The solid circle represents the critical point

mole weight of the repeat unit of the pseudocomponent and the thermoplastic, respectively. Note that for the thermoplastic the adjusted value, from equation (17), was used. The resulting values for n_1 and n_2 were 0.056 and 2.222, respectively, based on an N_{lin} value of 16.869.

The deuterated phase diagram can be estimated, in *Figure 4* from equation (18), in the familiar terms of temperature *versus* composition.

Notice the set of coexistence curves which give the compositions of the resulting phases, once phase separation has started. As mentioned before, a unique set of coexistence curves exists for each composition. The thermoplastic-rich branch of the coexistence curves lies within the spinodal region; the phase diagram corresponding to that phase is different to the bulk phase due to the different MWD of the epoxy when compared to the bulk. During phase separation, as the molecular weight of the epoxy increases, the phase diagram will move downwards and cross the temperature at which the blend cures, thereby inducing phase separation.

THE PHASE SEPARATION PROCESS

Having measured the MWD of the pseudocomponent

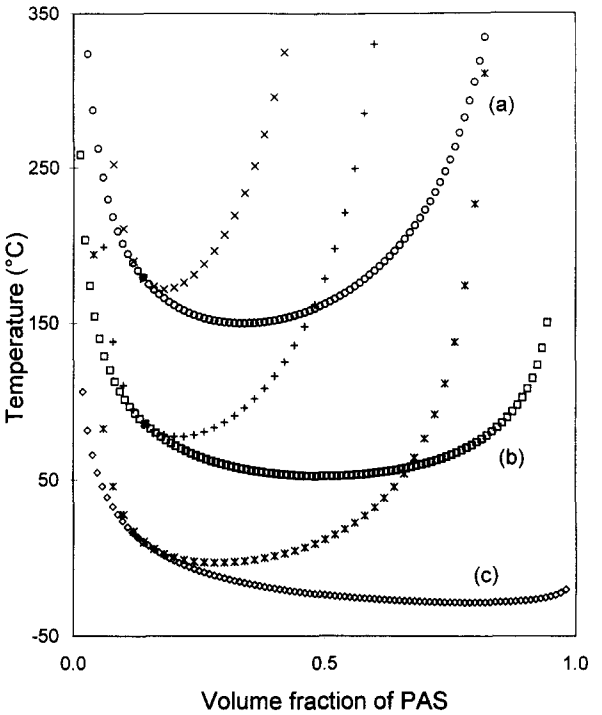

Figure 5 Predicted phase diagram evolution during cure for an epoxy/PAS/DDS 47/30/23 wt% blend after (a) 28 min, (b) 35 min and (c) 52 min of cure. Solid circles represent critical points

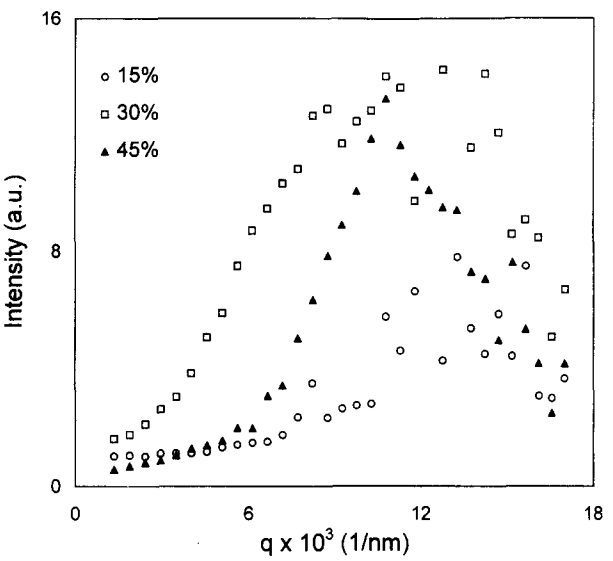

Figure 6 SALS scattering profiles of blends containing 15, 30 and 45 wt% of deuterated thermoplastic, at the end of phase separation

at different times during cure and assuming that the temperature dependence of the interaction parameter is the same for both deuterated and hydrogenous thermoplastic, we can now estimate, in *Figure 5*, the phase diagram evolution of the thermoplastic/thermoset blend. The downward shift of the phase diagram is predicted as well as the broadening of the metastable region[11].

In order to test the model, a series of light-scattering experiments and SEM studies were performed. Samples with compositions of 15, 30 and 45 wt% of d-PAS (the epoxy/4,4′-DDS ratio remained constant) were cast on microscope cover-slips following the same preparation route as for the SANS experiments. These were then cured under SALS observation following the temperature programme of the hydrogenous samples, as described in *Table 2*. *Figure 6* shows the light-scattering

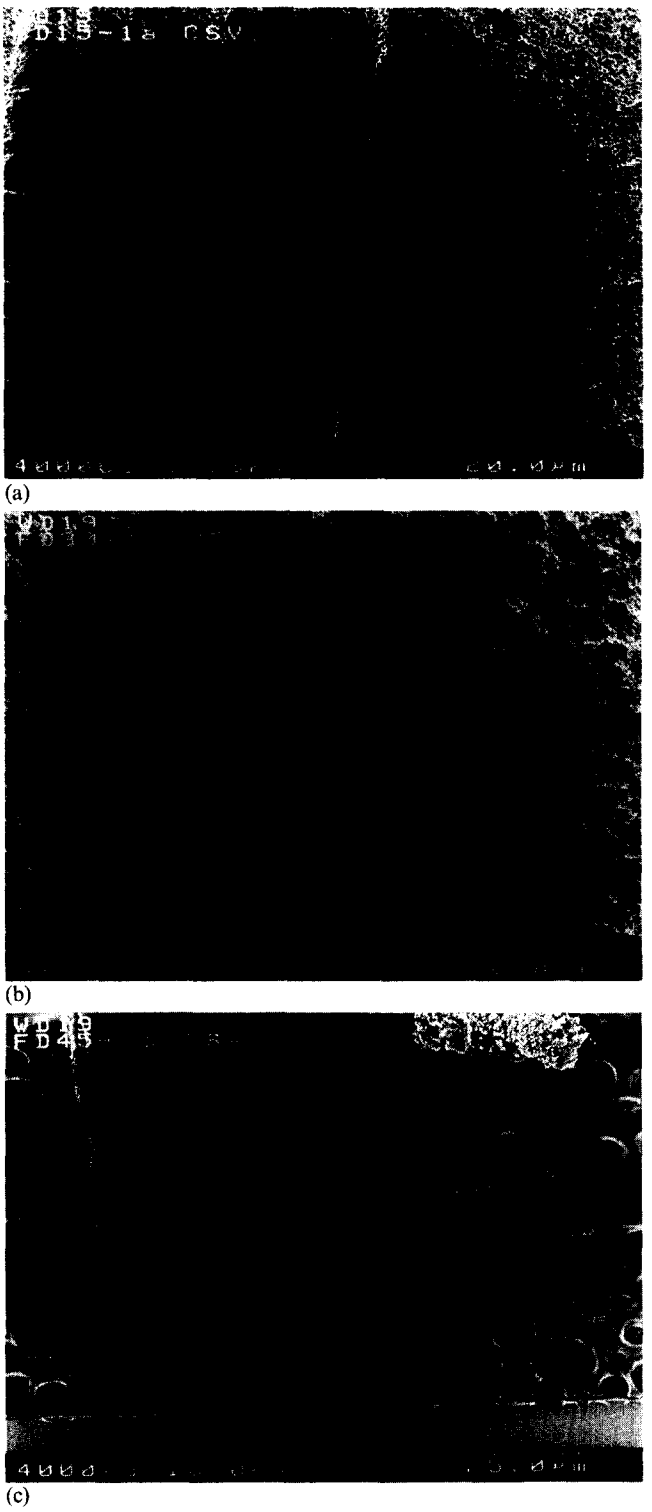

Figure 7 SEM micrographs of fractured and etched samples containing (a) 15, (b) 30 and (c) 45 wt% of d-PAS

profiles at the end of the experiment for the three compositions containing deuterated thermoplastic. It was not possible to observe phase separation in real time, probably due to the small refractive index difference between the thermoplastic and the epoxy[52]. However, both the relative intensity (30% > 45% > 15%) and the position of the peaks, in terms of q(30% < 45% < 15%), indicate that the phase separation process is spinodal decomposition which has progressed further for the 30% blend than for the other two. This observation is in good agreement with the predicted phase diagram in *Figure 4*, as the phase diagram shift towards lower temperatures during curing will cause the 30% blend to be deeper inside the spinodal region, followed by the 45% and the 15% blends.

The cured SALS samples were subsequently fractured and etched with a 1% solution of potassium permanganate in a 5:2:2 volume mixture of concentrated sulfuric acid/phosphoric acid/distilled water. After etching, the samples were sequentially washed in aqueous sulfuric acid, hydrogen peroxide (100 volumes), water and finally acetone. All samples were then sputter coated with platinum before SEM examination. The SEM micrographs exhibit a co-continuous structure for the 30 and 15% blends while those of the 45% blend exhibit a particulate structure with secondary phase separation inside the spherical domains (*Figure 7*). This is not surprising as the 45% blend has to cross a wider metastable region compared to the other two compositions. We suggest phase separation first proceeded via nucleation and growth in the metastable gap until the emerging particle phase, which is also simultaneously cross-linking and therefore has changing stability requirements, crossed its own spinodal and secondary phase separation occurred. That the secondary separation is spinodal decomposition suggests that the composition of the emerging particle phase is close to the critical composition[11]. This secondary phase separation may also be responsible for the intensity peak in the light-scattering experiments.

CONCLUSIONS

Using a simple model it was possible to predict the phase diagram of a curing thermoset/thermoplastic blend. The calculated phase diagram predictions were in good agreement with results from SALS and SEM experiments on the same blend. In addition, the model predicted, with relative success, the secondary phase separation which is often evident in thermoset/thermoplastic blends. A major assumption incorporated in this model, namely the validity of equation (1) in describing the MWD of the branched polymer, has not been tested explicitly. A more complete and reliable method for measuring the MWD would be required before this is possible. An obvious refinement to the model would be to incorporate polydispersity for the linear component to bring the predictions closer to real blends. In particular this will increase the size of the metastable region at low concentrations of thermoplastic.

We believe that this model will greatly improve our ability to predict the phase behaviour of complex blends, limiting the need for exhaustive experiments over the whole compositional range in order to accurately estimate the phase diagram of a particular blend. It will also enable determination of the curing conditions necessary for producing desired morphologies, and therefore properties, in applications of thermoset/thermoplastic blends.

ACKNOWLEDGEMENTS

We thank ICI plc for financial support (N.C., S.E.), provision of materials, test facilities and overall support. Thanks are also due to LOQ instrument scientists at the ISIS pulsed neutron source at Rutherford Appleton Laboratory for technical assistence in the SANS experiments.

REFERENCES

1. Bucknall, C. B., Partridge, I. K. and Phillips, M. J., *Polymer*, 1991, **32**, 786.
2. Jenkins, S. D., McGrail, P. T., Street, A. C. and Morrison, J. D., 6th International Conference on Crosslinked Polymers, Noordwijk, Holland, 1992.
3. Sefton, M. S., McGrail, P. T., Peacock, J. A., Wilkinson, S. P., Crick, R. A., Davies, M. and Alwen, G., 19th International SAMPE Technical Conference, 13–15 October, 1987.
4. Paul, D. R. and Newman, S., *Polymer Blends I.* Academic Press, London, 1978, p. 152.
5. Cahn, J. W., *Trans. Met Soc. AIME*, 1968, **242**, 166.
6. Cahn, J. W., *Acta Met.*, 1961, **9**, 795.
7. Inoue, T. and Ougizawa, T., *J. Macromol. Sci.-Chem.*, 1989, **1**, 147.
8. Hashimoto, T., Itakura, M. and Hasegawa, H., *J. Chem. Phys.*, 1986, **85**, 6118.
9. Binder, K. and Frisch, H. L., *J. Chem. Phys.*, 1984, **84**, 2126.
10. Williams, R. J. J., Borrajo, J., Adabbo, H. E. and Rojas, A. J., *Abs. Am. Chem. Soc.*, 1983, **186**, 96.
11. Clarke, N., McLeish, T. C. B. and Jenkins, S. D., *Macromolecules*, 1995, **28**, 4650.
12. Koningsveld, R. and Staverman, A. J., *J. Polym. Sci. A2*, 1968, **6**, 325.
13. Solc, K., *Macromolecules*, 1970, **3**, 665.
14. Solc, K., *Macromolecules*, 1973, **6**, 819.
15. Stauffer, D., *Introduction to Percolation Theory.* Taylor & Francis, London, 1985.
16. Flory, P. J., *Principles of Polymer Chemistry.* Cornell University Press, Ithaca, 1953.
17. Stauffer, D., Coniglio, A. and Adam, M., *Adv. Polym. Sci.*, 1982, **44**, 103.
18. Scott, R. L. and Magat, M., *J. Chem. Phys.*, 1945, **13**, 172.
19. Clarke, N., Theoretical aspects of linear branched polymer blends. Ph.D. thesis, University of Sheffield, 1994.
20. Riccardi, C. C., Borrajo, J., Williams, R. J. J., Girard-Reydet, E., Sauterau, H. and Pascault, J. P., *J. Polym. Sci. B: Polym. Phys.*, 1996, **34**, 349.
21. Stockmayer, W. H., *J. Polym. Sci.*, 1952, **9**, 69.
22. Stockmayer, W. H., *J. Polym. Sci.*, 1953, **11**, 424.
23. Peniche-Covas, C. A. L., Dev, S. B., Gordon, M., Judd, M. and Kajiwara, K., *J. Chem. Soc., Faraday Disc.*, 1974, **57**, 165.
24. Higgins, J. S. and Maconnachie, A., *Meth. Exp. Phys.*, 1987, **23**, 287.
25. Springer, T., *Springer Tracts Modern Phys.*, 1977, **64**.
26. Shibayama, M., Yang, H., Stein, R. S. and Han, C. C., *Macromolecules*, 1985, **18**, 2179.
27. Herkt-Maetzky, J. and Shelton, C., *J. Phys. Rev. Lett.*, 1983, **51**, 896.
28. Yang, H., Shibayama, M., Stein, R. S. and Han, C. C., *Polym. Bull.*, 1984, **12**, 7.
29. Patterson, D., Bhattacharyya, S. N. and Picker, P., *Trans. Faraday Soc.*, 1968, **64**, 648.
30. Squires, G. L., *Thermal Neutron Scattering*, Cambridge University Press, Oxford, 1978.
31. Higgins, J. S. and Bênoit, H. C., *Polymers in Neutron Scattering.* Clarendon Press, Oxford, 1994.
32. Higgins, J. S. and Stein, R. S., *J. Appl. Crystallogr.*, 1978, **11**, 346.
33. Binder, K., *J. Chem. Phys.*, 1983, **79**, 6387.
34. DeGennes, P. G., *Scaling Concepts in Polymer Physics.* Cornell University Press, New York, 1979.
35. Warner, M., Higgins, J. S. and Carter, A. J., *Macromolecules*, 1983, **16**, 1931.
36. Higgins, J. S., in *Polymer Blends and Mixtures*, ed. D. J. Walsh, J. S. Higgins and A. Maconachie, *NATO ASI Series.* Martinus Nijhoff, Dordrecht, 1984, p. 69.
37. Maconnachie, A., Fried, J. R. and Tomlins, P. E., *Macromolecules*, 1989, **22**, 4606.
38. Clark, J. N., Fernandez, M. L., Tomlins, P. E. and Higgins, J. S., *Macromolecules*, 1993, **26**, 5897.
39. Zimm, B. H., *J. Chem. Phys.*, 1948, **16**, 1093.
40. Heenan, R. K. and King, S. M., *Proceedings of the International Seminar on Structural Investigations at Pulsed Neutron Sources*, Dubna, Russia, September 1992.
41. ISIS, *User Guide Experimental Facilities at ISIS.* RAL-88-030. Rutherford Appleton Laboratory, Oxfordshire, 1988.
42. Kim, B. S., Chiba, T. and Inoue, T., *Polymer*, 1995, **36**, 43.
43. Cracknell, G. and Akay, M., *J. Therm. Anal.*, 1993, **40**, 565.
44. Akay, M. and Cracknell, G., *J. Appl. Polym. Sci.*, 1994, **52**, 663.
45. Mondragon, I. and Bucknall, C. B., *Plastics Rubber Composites*, 1994, **21**, 275.
46. Grillet, A. C., Galy, J. and Pascault, P., *Polymer*, 1989, **30**, 2094.
47. Takenaka, M. and Hashimoto, T., *Macromolecules*, 1994, **27**, 6117.
48. *LOQ Users' Manual.* Rutherford Appleton Laboratory, Oxfordshire, 1988.
49. Wignall, G. D. and Bates, F. S., *J. Appl. Crystallogr.*, 1987, **20**, 28.
50. Sears, V. F., *Neutron News*, 1992, **3**, 26.
51. Han, C. C., Bauer, B. J., Clark, J. C., Muroga, Y., Matsushita, Y., Okada, M., Tran-cong, Q., Chang, T. and Sanchez, I. C., *Polymer*, 1988, **29**, 2002.
52. Kim, B. S., Chiba, T. and Inoue, T., *Polymer*, 1995, **36**, 67.